

## Rare Earth Dopant Effects on Optical Properties of Alumina: DFT Study

M. S. MAHABAL<sup>1</sup>, Dr. M. D. DESHPANDE<sup>1\*</sup>

<sup>1</sup>Department of Physics, H. P. T. Arts & R. Y. K. Science College, Nasik-5.

\*Corresponding author email: d\_mrinal@yahoo.com

### ABSTRACT

The optical properties of rare earth (RE) doped alumina,  $RE_xAl_{2-x}O_3$  ( $RE = Ce, Nd, Gd$  and  $x = 0.1, 0.3$ ) have been studied using first principles calculations. We have made the comparison between the electronic and optical properties of RE doped  $\alpha$ - and  $\gamma$ - $Al_2O_3$ . The substitution of Al atoms with RE atoms is favorable in both the phases of alumina. RE doping induces large magnetic moments in both the nonmagnetic phases of alumina. When RE atom is incorporated in  $Al_2O_3$  matrix the band gap structure is modulated substantially and the levels from RE atom get inserted near Fermi level of  $Al_2O_3$  which effectively decreases the band gap. With an increase in the concentration of RE element red shift is observed in the optical spectra as compared to that of host system. The static dielectric constant and refractive index of  $\alpha$ - and  $\gamma$ - $Al_2O_3$  increases with an increase in concentration of RE element. Among Ce, Nd and Gd doped systems, it is concluded that only Gd doped  $\gamma$ - $Al_2O_3$  preserves the size of the band gap at the same time elevates the dielectric constant of  $\gamma$ -phase. Gd doped alumina can serve as a promising candidate for an alternative gate oxide material in semiconductor technology.

**Keywords:** Density Functional Theory, Optical Properties, Rare earth doped Alumina.

### INTRODUCTION

Alumina ( $Al_2O_3$ ) is one of the most versatile ceramics, utilized in an amazing range of structural and optical applications. It has many industrial applications such as catalysis, coatings, microelectronics, optical materials, and advanced material technology.<sup>1</sup> It can crystallize in different crystal structures depending on the growth conditions. The  $\alpha$ - $Al_2O_3$  can only be formed at temperatures higher than 1000°C; at lower temperatures only the metastable  $Al_2O_3$  polymorph phases can be synthesized. The sapphire ( $\alpha$ - $Al_2O_3$ ) is the most stable and hard phase, and is used for ultra-hard coatings. Among the various phases, the  $\gamma$ - $Al_2O_3$  can be formed at low temperature, greater than 350°C. It is one of the important material in microelectronic processing<sup>2</sup> due to its porous structure, high surface area and high catalytic surface activity.

The semiconductor industry which constantly searches for new materials to build dielectric gates in transistors and integrated circuits. Various studies indicate the alumina as one of the most proper candidates for high-k gate dielectric for such an employment after  $SiO_2$ .<sup>3</sup> It has a wide band gap (8.8 eV), similar band offset as the  $SiO_2$  and high dielectric constant (~9), which can be elevated even more by appropriate doping of the pure material. While enhancing the dielectric constant with suitable dopant the main constraint is that the band gap and the band offset of host material should not change too much. Theoretically,<sup>4</sup> and experimentally<sup>5</sup> it is seen that the presence of certain transition metals (TM), Y and Sc within  $\alpha$ - $Al_2O_3$  phase maintains the gap value and increases the dielectric constant, while the presence of others (Zr, Nb) diminishes the gap and dampen the dielectric properties of the host. It is seen that incremental doping of  $Al_2O_3$  by TM can serve higher dielectric constant without bandgap degradation. These theoretical and experimental results encourage us further to study electronic and optical properties of rare earth doped alumina and predict its applicability as a high-k dielectric material.

Today, most optical materials rely on RE rather than TM dopants because RE doping produces greater efficiencies and lower lasing thresholds. RE-doped alumina could provide an extremely versatile ceramic, opening the door for a host of new applications and devices. Although significant experimental work has been done to study the effect of RE dopants in some ceramic systems,<sup>1,2</sup> Al<sub>2</sub>O<sub>3</sub> has not been explored. RE elements exhibit unique electronic, magnetic and optical properties, primarily governed by the occupancy of 4f shell. The presence of 4f shell and the large size influence the local structure, stability and magnetic properties of the host material. Limmer et. al.<sup>6</sup> have studied the structural and magnetic properties of Pr, Nd, Gd, Er, and Yb doped  $\alpha$ -Al<sub>2</sub>O<sub>3</sub> and  $\theta$ -Al<sub>2</sub>O<sub>3</sub> phases. It is observed that increasing number of unpaired number of electrons decreased the defect formation energy and increased the local magnetic moments, suggesting that RE dopants may significantly affect the processing of Al<sub>2</sub>O<sub>3</sub> under magnetic field. These earlier reports studied the relationship between dopant concentration, phase stability and magnetic properties using RE dopants. To our knowledge, there are very few theoretical<sup>7</sup> as well as experimental<sup>8-11</sup> studies in determining the optical properties with RE doped alumina. The optical properties of  $\alpha$ -Al<sub>2</sub>O<sub>3</sub> and La doped  $\alpha$ -Al<sub>2</sub>O<sub>3</sub><sup>7</sup> have been studied by using density functional study (DFT). It is observed that the refractive index of  $\alpha$ -Al<sub>2</sub>O<sub>3</sub> increases with the substitution of La for Al. Based on these earlier reports, our aim is to understand the influence of RE elements on the electronic and optical properties of alumina effectively to focus on its application as a high-k dielectric gate material. In this work, we studied the electronic and optical properties of RE doped alumina, RE<sub>x</sub>Al<sub>2-x</sub>O<sub>3</sub> where RE = Ce, Nd, and Gd and x = 0.1 and 0.3. As noted earlier about the role of  $\alpha$ - and  $\gamma$ -Al<sub>2</sub>O<sub>3</sub> phases in semiconductor industry, in this study we have considered  $\alpha$ - and  $\gamma$ - phases of alumina. This study will help to enhance the understanding of how the RE dopant affects the band gap and dielectric properties of various phases of alumina, and also the study will contribute in further development of alumina based high-k materials. It is observed that doping of RE atom is favorable in both the phases of alumina. Ferromagnetic coupling is observed between the RE atoms. With the increase in number of RE concentration, the red shift is observed in the optical spectrum along with the enhancement in dielectric constant of alumina.

## COMPUTATIONAL DETAILS

All the calculations are performed by using density functional theory as implemented in Vienna *Ab Initio* Simulation Package (VASP).<sup>12</sup> The ionic potentials are represented by projector augmented wave (PAW) potentials and the exchange correlation energy is represented by a generalized gradient approximation (GGA) functional proposed by Perdew, Burke, and Ernzerhof (PBE).<sup>13</sup> For  $\alpha$ -Al<sub>2</sub>O<sub>3</sub> the supercell consist of the 6 units of Al<sub>2</sub>O<sub>3</sub> and for  $\gamma$ -Al<sub>2</sub>O<sub>3</sub> the supercell consisting of 8 units. We have used a (6x6x1) Monkhorst-Pack<sup>14</sup> k-point sampling for Brillouin zone integration. The cutoff energy for plane wave was set to 282.8 eV. The calculations are considered to be converged when the forces on each ion was 0.001 eV/Å with the convergence in the total energy of about 10<sup>-4</sup> eV. In this study, we have considered RE dopant, Ce, Nd and Gd with x = 0.1 and 0.3 in bulk alumina. For x = 0.1, the single Al atom is substituted by a RE atom. For x = 0.3, two Al atoms are substituted by RE atoms. To find out lowest energy configurations we have considered tetrahedral and octahedral sites as well as various distances between the two RE atoms. In the standard mode, VASP performs a fully relativistic calculation for the core-electrons and treats valence electrons in a scalar relativistic approximation. The DFT calculations including the spin-orbit coupling are carried out for both the undoped and doped phases. The calculations included for l = 3, l = 2 and l = 1 orbitals in spin-orbit operator ( $\hat{H}_{S.O.}$ ).

The optimized configurations are used to calculate the optical properties. The frequency dependent dielectric matrix was calculated using VASP 5.2 optical program. The frequency

dependent dielectric matrix calculations are carried out by increasing the number of states by a factor of 3. It is calculated using summation over conduction band method for self-consistent dielectric function evaluated from density functional perturbation theory within linear response theory.<sup>15</sup> From the optical spectra we have calculated the static dielectric constant and refractive index for undoped and RE doped systems.

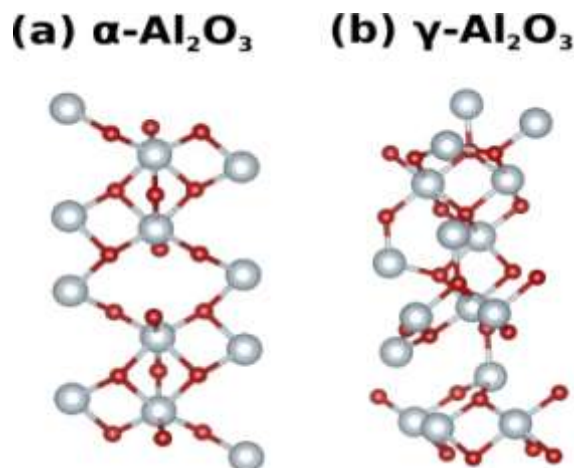


**Fig. 1 :** Schematic representation of (a)  $\alpha$ - $\text{Al}_2\text{O}_3$  and (b)  $\gamma$ - $\text{Al}_2\text{O}_3$  unit cells. The gray spheres represent the Al atoms and red spheres represent the O atoms.

To benchmark the modeling elements of the computational method employed in this study, we have first considered  $\alpha$ - and  $\gamma$ - $\text{Al}_2\text{O}_3$  phases. Figure 1(a) and (b) shows the unit cell configuration for both  $\alpha$  and  $\gamma$ - $\text{Al}_2\text{O}_3$  phases. The  $\alpha$ - $\text{Al}_2\text{O}_3$  consist with 6 unit cells consist of 30-atoms (Al-12 and O-18) whereas for  $\gamma$ - $\text{Al}_2\text{O}_3$  we have used 8 unit cells consists of 40-atoms (Al-16 and O-24). The calculated lattice parameters for  $\alpha$ - $\text{Al}_2\text{O}_3$  are  $a = b = 4.16 \text{ \AA}$ ,  $c = 13.12 \text{ \AA}$ . These compare well with the experimental<sup>16</sup> values of  $a = b = 4.76 \text{ \AA}$ ,  $c = 12.99 \text{ \AA}$ . The calculated lattice parameters for  $\gamma$ - $\text{Al}_2\text{O}_3$  are  $a = 5.45 \text{ \AA}$ ,  $b = 5.40 \text{ \AA}$ ,  $c = 13.68 \text{ \AA}$  agree well with the previously<sup>17</sup> calculated values of  $a = 5.61 \text{ \AA}$ ,  $b = 5.57 \text{ \AA}$ ,  $c = 13.48 \text{ \AA}$ . In spinel  $\gamma$ - $\text{Al}_2\text{O}_3$ , Al atoms are tetrahedrally and octahedrally coordinated, and oxygen are tetracoordinated. Table 1 depicts the average Al-O bond length, cohesive energy, magnetic moment, and band gap for  $\alpha$ - and  $\gamma$ -phase. Stability analysis shows that the  $\alpha$ -phase has higher stability as compared to  $\gamma$ -phase. For  $\alpha$ - $\text{Al}_2\text{O}_3$ , the Al-O bond distances are in the range of  $1.85 - 1.98 \text{ \AA}$ . Those are similar to the experimental bond lengths ( $1.86 - 1.97 \text{ \AA}$ ). The  $\alpha$ - and  $\gamma$ -phase are found to be non-magnetic. The calculated band gap of  $\alpha$ - $\text{Al}_2\text{O}_3$  is 6.1 eV. It is to be noted that the experimental band gap of bulk alumina is 8.8 eV.<sup>18</sup> The underestimation of the calculated band gap is due to the use of GGA.<sup>12</sup> The calculated band gap for  $\gamma$ - $\text{Al}_2\text{O}_3$  is 3.80 eV and calculations by Ahuja et. al.<sup>19</sup> showed the band gap 3.9 eV while the experimental band gap for the  $\gamma$ - $\text{Al}_2\text{O}_3$  is 7.0 eV.<sup>20</sup> The calculated results in terms of structural stability and electronic properties of  $\alpha$ - and  $\gamma$ -phase are in excellent agreement with the earlier studies<sup>4,7,21-24</sup> indicating the accuracy and reliability of the modeling elements used in this study.

## RESULTS AND DISCUSSION

As discussed earlier, our interest is to understand optical properties of  $\alpha$ - and  $\gamma$ -phase RE doped alumina where RE = Ce, Nd, and Gd. The ionic radius of Ce, Nd and Gd atom ( $1.89 \text{ \AA}$ ,  $1.12 \text{ \AA}$ , and  $1.07 \text{ \AA}$ , ) are larger than that of Al atom ( $0.57 \text{ \AA}$ ). Substitutional doping of RE element whose ionic radii are larger than that of Al atom on Al site expands the lattice parameters by  $\sim 0.5\%$  and also enhanced the local structural distortion around the substitutional Al site. With the RE doping

large variation in Al – O bond lengths are observed for  $\alpha$ -phase as compare to that of  $\gamma$ -phase. The effect of doping on the stability of  $\alpha$ - and  $\gamma$ -phases is determined by calculating the cohesive energy for the pure and doped supercell of alumina. For  $\alpha$ -Al<sub>2</sub>O<sub>3</sub> and RE<sub>x</sub>Al<sub>2-x</sub>O<sub>3</sub>, the cohesive energy, E<sub>coh</sub> is given by :

$$E_{coh} = [E(A_{12}O_{18}) - [12 E(Al) + 18 E(O)]] / 30 \quad (1)$$

$$E_{coh} = E(REAl_{11}O_{18}) - [E(RE) + 11 E(Al) + 18 E(O)] / 30 \quad \text{for } x = 0.1 \quad (2)$$

$$E_{coh} = E(RE_2Al_{10}O_{18}) - [2 E(RE) + 10 E(Al) + 18 E(O)] / 30 \quad \text{for } x = 0.3 \quad (3)$$

Similarly the E<sub>coh</sub> is calculated for  $\gamma$ - undoped and RE doped alumina. The calculated bond lengths, cohesive energy, magnetic moments with RE doping in alumina are presented in Table 1.

**Table 1:** Average bond distances (Al-O, RE-O, and RE-RE (Å)), Cohesive Energy (E<sub>coh</sub> (eV/atom)), Magnetic Moment ( $\mu$ B), and Band gap (E<sub>g</sub> (eV)) for RE<sub>x</sub>Al<sub>2-x</sub>O<sub>3</sub> systems where RE = Ce, Nd, and Gd and x = 0.1 and 0.3 along with undoped  $\alpha$ - and  $\gamma$ -alumina.

	$\alpha$ -RE <sub>x</sub> Al <sub>2-x</sub> O <sub>3</sub>						$\gamma$ -RE <sub>x</sub> Al <sub>2-x</sub> O <sub>3</sub>							
		RE = Ce		Nd		Gd			RE = Ce		Nd		Gd	
x	0	0.1	0.3	0.1	0.3	0.1	0.3	0	0.1	0.3	0.1	0.3	0.1	0.3
Al-O	1.8 5	1.8 7	1.90	1.9 1	1.93	1.9 7	1.99	1.8 0	1.8 2	1.8 3	1.8 5	1.8 6	1.7 9	1.85
RE-O	-	2.2 4	2.20	2.2 1	2.12	2.2 6	2.13	-	2.1 0	2.1 1	2.1 2	2.0 9	2.0 6	2.31
RE-RE	-	-	12.8 9	-	12.9 5	-	12.9 7	-	-	3.3 6	-	3.3 1	-	3.67
E <sub>coh</sub>	6.4 1	6.3 5	6.38	6.3 5	6.32	6.5 3	6.49	6.3 6	6.3 5	6.3 0	6.3 7	6.3 2	6.4 9	6.44
$\mu$ B	0	1	2	3	6	7	14	0	1	2	3	6	7	14
E <sub>g</sub>	6.1 0	0.1	0.26	0.5 6	0.31	3.3 3	3.11	3.8	0.1 9	0.2 0	0.2 4	0.3 6	3.3 8	4.32

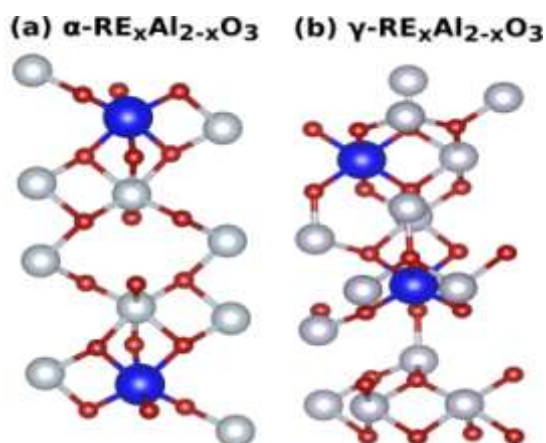


**Fig. 2:** The unit cell of (a)  $\alpha$ -RE<sub>x</sub>Al<sub>2-x</sub>O<sub>3</sub> and (b)  $\gamma$ -RE<sub>x</sub>Al<sub>2-x</sub>O<sub>3</sub> (x = 0.3) used in the study. The gray spheres represent the Al atoms, red spheres represent the O atoms, and blue spheres represent the RE atoms where RE = Ce, Nd and Gd.

The atomic size mismatch appears to be the origin of slightly lowering the stability of Ce and Nd doped alumina. As the size difference between Al and Gd decreases the stability of Gd doped alumina increases as compared to that of pure alumina. It is found that with an increase in RE concentration the ferromagnetic behavior is observed in both the phases. Limmer et. al.<sup>6</sup> investigated structural and magnetic properties of Nd and Gd doped  $\alpha$ - and  $\theta$ -alumina. The calculated magnetic moments for Ln doped  $\alpha$ - and  $\theta$ -alumina in octahedral and tetrahedral sites for Nd and Gd doping are  $\sim 2.94$  and  $6.87 \mu_B$ , respectively. Our calculations show that for both the phases of alumina with Nd and Gd doping the magnetic moments are 3 and  $7\mu_B$ , respectively. All these results indicate that the magnetic moments are independent of phase and dopant site. The magnetic moment is correlated with the number of unpaired electrons of the RE element. The calculated band gap from the band structure (not shown) calculations are mentioned in Table 1. When RE atom is incorporated in  $Al_2O_3$  matrix the band gap structure is modulated substantially and the levels from RE atom get inserted near Fermi level of  $Al_2O_3$  which effectively decreases the band gap. For Ce and Nd doped systems the band gap decreases drastically for both the phases of alumina. With the Gd doping the band gap of  $\alpha$ - $Al_2O_3$  decreases from 6.1 to 3.11 eV but for  $\gamma$ - $Al_2O_3$  slight increase in the band gap is observed. Due to large variations in the band gap of the RE doped alumina some effects on optical properties of  $\alpha$ - and  $\gamma$ - $Al_2O_3$  are highly expected.

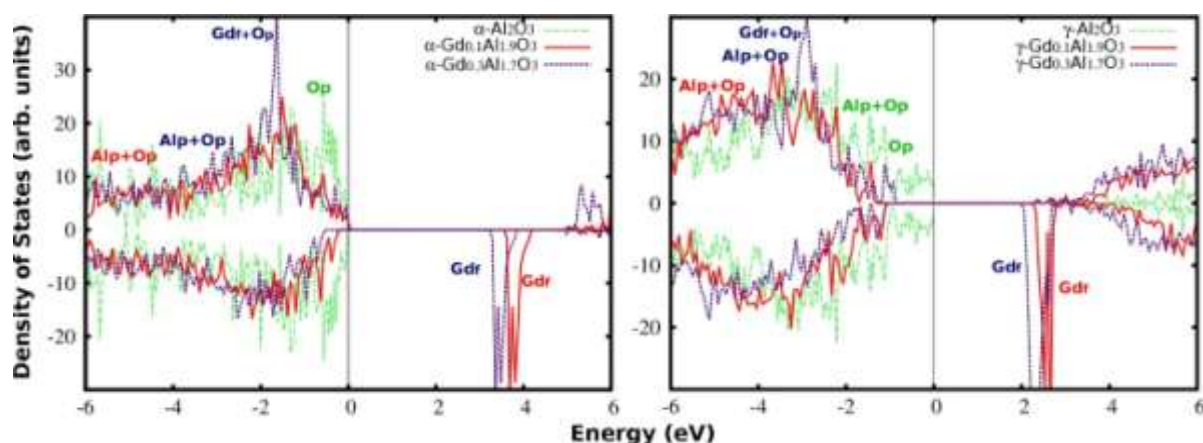


**Fig. 3:** Total density of states of Gd doped  $\alpha$ - and  $\gamma$ - $Al_2O_3$  for  $x = 0.1$  and  $0.3$ . Green spectra represent TDOS for  $\alpha$ - and  $\gamma$ - $Al_2O_3$ . The labels indicate the contributions of a particular atom state to the total density of states. The Fermi level is aligned to zero.

To understand the variations in the band gap we have also calculated the total density of states (TDOS) for RE doped  $\alpha$ - and  $\gamma$ - $Al_2O_3$  and compared with both undoped phases of alumina. As noted earlier, Ahuja et. al.<sup>19</sup> reported the density functional calculations of the electronic structure of  $\gamma$ - $Al_2O_3$  system and made a comparison between  $\alpha$ - and  $\gamma$ - phases of alumina. We have calculated the projected DOS on RE, Al and O atom. Our calculated TDOS for  $\alpha$ - and  $\gamma$ - $Al_2O_3$  systems show the similar nature reported by earlier study.<sup>19</sup> When RE atom is incorporated in  $Al_2O_3$  matrix the total DOS are modulated substantially and the levels from RE atom get inserted near Fermi level of  $Al_2O_3$  which effectively decreases the band gap. Here, as a representative we have shown the TDOS for Gd doped  $\alpha$ - and  $\gamma$ - $Al_2O_3$  systems along with the corresponding  $\alpha$ - and  $\gamma$ -alumina (Figure 3). The difference between the spin up and spin down states shows the magnetic behavior of the Gd doped alumina systems. The TDOS for  $Gd_xAl_{2-x}O_3$  ( $x = 0.3$ ) show the delocalized nature as compared to the host. Overall, the broadening of the spectra reflects the increase in degree of hybridization in RE doped

systems. It is observed that with the substitution of Al atoms by RE, the defects in both the phases increase the number of newly populated energy levels in RE doped  $\alpha$ - and  $\gamma$ -Al<sub>2</sub>O<sub>3</sub>. For RE doped  $\alpha$ - phase, the lower energy spectra is contributed by Al-s states, the middle level spectra from the Al-p and O-p states. The spectra below the Fermi is dominated by the contribution from O-p states. The spectra near the Fermi level is mainly dominated by the RE-f states. It is also seen that the spectra is shifted towards the Fermi level with the increase in concentration from 0.1 to 0.3. The shift in total DOS may leads to the red shift in the optical spectra.

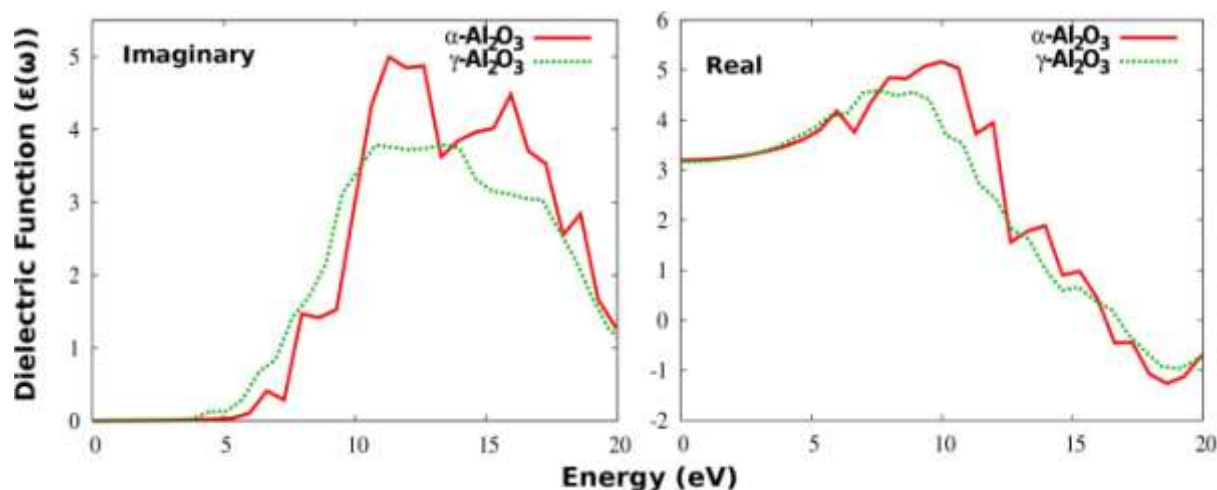


**Fig. 4:** The calculated imaginary and real part of dielectric function (along x) for  $\alpha$ -Al<sub>2</sub>O<sub>3</sub> and  $\gamma$ -Al<sub>2</sub>O<sub>3</sub>. The continuous line indicates the optical spectra of  $\alpha$ -Al<sub>2</sub>O<sub>3</sub> and dotted line for  $\gamma$ -Al<sub>2</sub>O<sub>3</sub>.

In Figure 4, we present the imaginary and real parts of dielectric function for  $\alpha$ - and  $\gamma$ -Al<sub>2</sub>O<sub>3</sub>. The imaginary and real dielectric values of the materials are plotted for all photon energies. The overall nature of optical spectra of  $\gamma$ -Al<sub>2</sub>O<sub>3</sub> is similar to the  $\alpha$ -phase. It is observed that the  $\gamma$ -Al<sub>2</sub>O<sub>3</sub> spectra is more smoother as compared to the  $\alpha$ -Al<sub>2</sub>O<sub>3</sub>. The first transition of  $\gamma$ -phase appears at lower energy range as compared to  $\alpha$ -phase. The first transition of  $\alpha$ -phase is appear near 6 eV, while in  $\gamma$ -phase the it is near to 4 eV. For  $\alpha$ - phase from the imaginary part two main peaks are observed around 11.5 and 16 eV where as for  $\gamma$ - phase two main peaks are around 9.8 and 14.5 eV. Ahuja et. al.<sup>19</sup> have calculated the real and imaginary part of the dielectric functions using full linear muffin-tin-orbital (FP-LMTO) method for  $\alpha$ - and  $\gamma$ -Al<sub>2</sub>O<sub>3</sub>. Our calculated results are similar with their results.

Further, we have calculated the real and imaginary parts of dielectric function along three directions for  $\alpha$ - and  $\gamma$ - RE<sub>x</sub>Al<sub>2-x</sub>O<sub>3</sub> where RE = Ce, Nd, and Gd and x = 0.1 and 0.3. Along y and z directions, the spectra show a similar nature as compared to the spectra along the x direction. In the spectra, the presence of multiple peaks is evidently seen along the x direction in the lower energy range. The imaginary and real parts of the dielectric functions along x directions for doped systems along with undoped alumina are shown in Figure 5. Except in lower energy range the nature of imaginary and real parts of dielectric function for RE doped alumina show a similar nature to those of  $\alpha$ - and  $\gamma$ - alumina. The doping of large size Ce in alumina matrix induces high intensity peak in the lower energy range of optical spectra. With decrease in size from Ce to Nd to Gd as compared to Al atom, the peak intensity decreases. The red shift of first transition peak and the increased number of transitions can be assigned to induced defects activated by RE elements. The red shift is more dominant for Ce and Nd doped alumina as compared to that of Gd doped alumina which reveals the decrease in the band gap for RE doped alumina systems. The intensity of lower energy peaks as well

as the shift in the spectra increases with the doping of RE elements. The optical spectra reflects the nature of the density of states of the system.

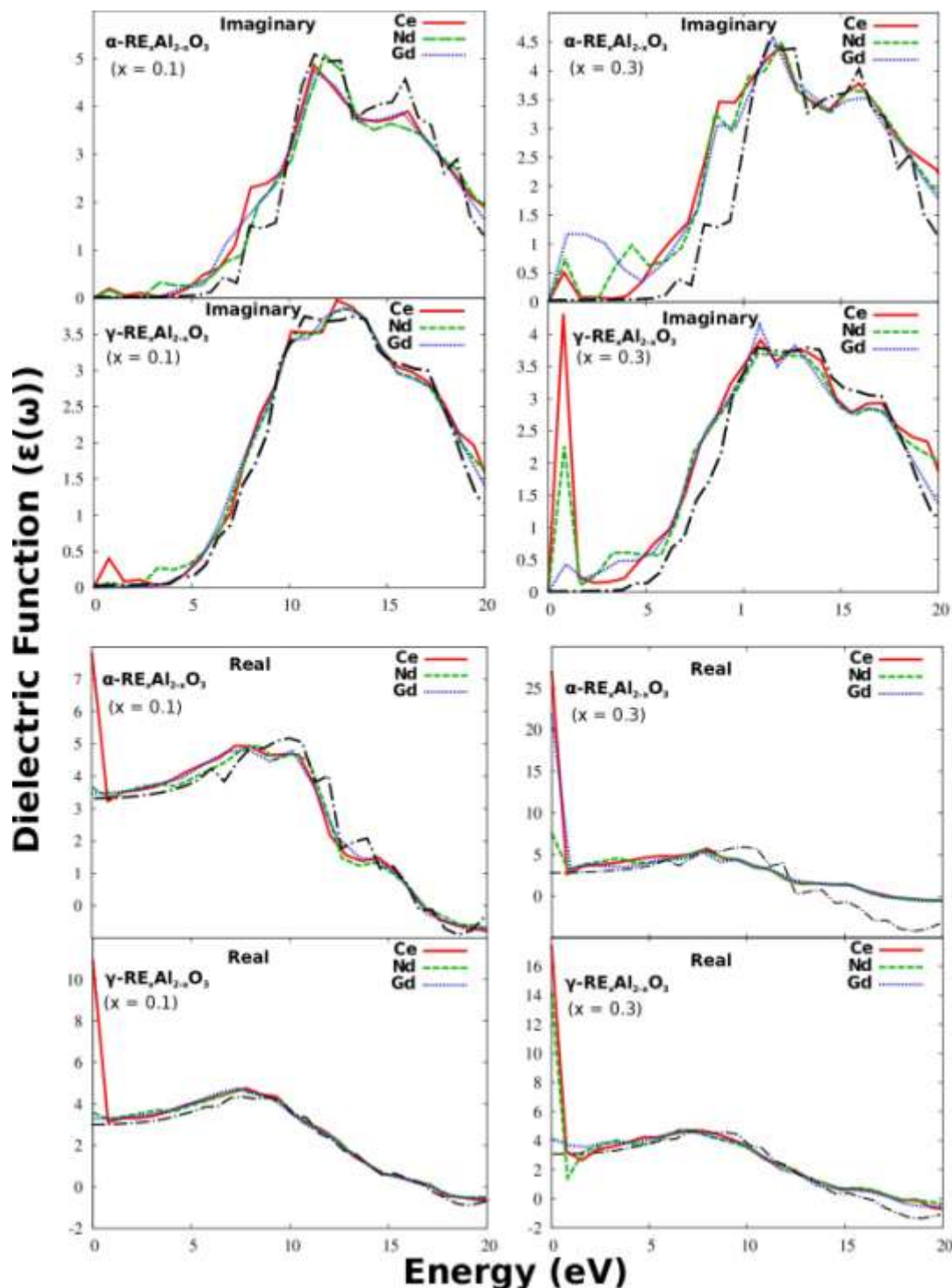


**Fig. 5 :** Imaginary and real part (along x direction) of dielectric function for  $\alpha$ - and  $\gamma$ -  $\text{RE}_x\text{Al}_{2-x}\text{O}_3$  where RE = Ce, Nd, and Gd and  $x = 0.1$  and  $0.3$ . Black line indicates the imaginary and real part of dielectric functions for  $\alpha$ - and  $\gamma$ - $\text{Al}_2\text{O}_3$  phase.

Overall with the substitution of Al atoms with RE atoms, the defects in both the phases further reduce the energy of newly populated level in  $\alpha$ - and  $\gamma$ - $\text{Al}_2\text{O}_3$ . The spectra of RE doped  $\alpha$ - and  $\gamma$ - $\text{Al}_2\text{O}_3$  are smoother as compared that of host phases. With the doping of RE atom, the dielectric

function in the spectrum is spread over a wide energy range, thus leading to broader spectrum. The broadening of the spectrum in higher energy range reflects the increase in degree of hybridization in RE doped alumina. The doping of RE atoms in  $\text{Al}_2\text{O}_3$ , the energy of the absorption edge shift towards the lower energy as compared to pure alumina.

**Table 2 :** Dielectric constant ( $\epsilon$ ) and refractive index ( $\eta$ ) for  $\alpha$ - and  $\gamma$ -  $\text{RE}_x\text{Al}_{2-x}\text{O}_3$  where RE = Ce, Nd, and Gd and  $x = 0.1, 0.3$  along with dielectric constant and refractive index for  $\alpha$ - $\text{Al}_2\text{O}_3$  and  $\gamma$ - $\text{Al}_2\text{O}_3$ .

	$\alpha$ - $\text{RE}_x\text{Al}_{2-x}\text{O}_3$							$\gamma$ - $\text{RE}_x\text{Al}_{2-x}\text{O}_3$						
		RE = Ce		Nd		Gd			RE = Ce		Nd		Gd	
x	0	0.1	0.3	0.1	0.3	0.1	0.3	0	0.1	0.3	0.1	0.3	0.1	0.3
$\epsilon$	3.31	7.9 2	27.4 1	3.77	7.7 2	3.49	22.2 2	3.25	11. 0	17.6 6	3.65	14.4 1	3.33	4.24
$\eta$	1.81	2.8 1	5.23	1.94	2.7 7	1.86	4.71	1.80	3.3 1	4.20	1.91	3.79	1.82	2.05

The optical behavior of a material is important to determine its usage in optical devices. A knowledge of the optical constants of a material, such as dielectric constant and refractive index is quite essential to examine the material potential in optical communication and designing optoelectronic devices. To understand the dielectric properties, we have calculated dielectric constant ( $\epsilon$ ), and refractive index ( $\eta$ ) from real part of dielectric function. The calculated optical constants are presented in Table 2. Basically, dielectric constant is the quantity that used to quantify the response of a material to an applied external electric field. The static dielectric constant is calculated as a zero energy limit of the real part of the dielectric tensor. The dielectric constants of  $\alpha$ - and  $\gamma$ - $\text{Al}_2\text{O}_3$  are 3.31 and 3.25, respectively. From the earlier results,<sup>19</sup> it is seen that dielectric constants are 3.2 and 3.0 for  $\alpha$ - and  $\gamma$ -phase. The experimental<sup>25</sup> value of the dielectric constant for  $\alpha$ -phase is 3.1. The refractive index of  $\alpha$ - and  $\gamma$ - $\text{Al}_2\text{O}_3$  are 1.81 and 1.80, respectively. Ahuja et. al.<sup>19</sup> investigated refractive index using FPLMTO method for  $\alpha$ - and  $\gamma$ -phases is 1.79 and 1.73, respectively. From KK analysis of EEL data<sup>18</sup> and Mo and Ching et. al.<sup>26</sup> found the refractive index for  $\alpha$ -phase is 1.78. The dielectric constant and refractive index are in good agreement with the previous results for  $\alpha$ - and  $\gamma$ -phases.<sup>4,7,19</sup> From the Table 2, it is found that for both the phases with RE doping the dielectric constant and refractive index of alumina increases.

As discussed earlier, the main goal of this work is to estimate if the doped material satisfy the fundamental criteria of semiconductor industry or not. The doped material should meet two basic criteria : (1) it must not change too much band gap of pure material nor the band offset around it and (2) it must enhance the dielectric constant in low energy range. From the analysis of the electronic structure (Table 1) and the optical properties (Table 2) of the pure and doped alumina, it is noted that Ce, Nd doped alumina show enhancement in dielectric constants but at the same time large reduction in bandgap as compare to the band gap size of  $\alpha$ - and  $\gamma$ - $\text{Al}_2\text{O}_3$ . For Gd doped  $\alpha$ - $\text{Al}_2\text{O}_3$  the band gap decreases from 6.1 to 3.11 eV, it maintains the semiconducting behavior of the system. The dielectric constant value increases from 3.31 to 22.22. In  $\gamma$ - phase, Gd doping preserves the size of the band gap of  $\gamma$ - $\text{Al}_2\text{O}_3$ . This is also confirmed from the optical spectra that the optical absorption edge for Gd doped alumina in  $\gamma$ - phase does not differ much from the absorption edge of pure  $\gamma$ - $\text{Al}_2\text{O}_3$ . At the same time the dielectric constant also increases. Among these three RE elements, only Gd doped alumina has a potential to be further development as a high-k dielectric material while Ce and Nd doped  $\alpha$ - and  $\gamma$ - $\text{Al}_2\text{O}_3$  do not have that potential. We hope that the rare earth doping with bulk alumina considered here would serve as reasonable model for gaining qualitative insight about the



optical properties of RE doped alumina. The present study should also provide relevant fundamental science to improve the design and application of alumina, in the field of optoelectronics and photovoltaics.

## CONCLUSIONS

We performed a theoretical study of the Ce, Nd and Gd doped  $\alpha$ - and  $\gamma$ -Al<sub>2</sub>O<sub>3</sub>. The electronic and optical properties of pure and the doped systems have been studied using density functional theory. There are two basic criteria concerning about doped material, the first one is the preservation of the band gap and second the elevation of dielectric constant value of the pure material. From the analysis of the electronic structure and optical properties of the pure and the RE doped alumina systems (RE = Ce, Nd and Gd), we would like to conclude that in case of Ce and Nd doped alumina for both the phases significant decrease of the band gap size and red shift in the optical spectra of alumina is observed. Due to this fact, the increase in dielectric constant loses its importance for Ce and Nd doped systems. Only Gd doped  $\gamma$ -Al<sub>2</sub>O<sub>3</sub> maintains the band gap with small variation at the same time the increase in dielectric constant is observed. Among Ce, Nd and Gd doped alumina, only Gd doped  $\gamma$ -Al<sub>2</sub>O<sub>3</sub> phase has a potential to serve as high-k dielectric material in semiconductor industry.

## ACKNOWLEDGMENTS

Authors acknowledges the Center for Development of Advance Computing (CDAC), Pune and Bangalore for providing the supercomputing facilities.

## REFERENCES

- [1] W. H. Gitzen, *Am. Ceram. Soc.*, 1970.
- [2] T. Perevalov, A. Shaposhnikov, V. Gritsenko, *Microelectron. Eng.*, 2009, 86, 1915.
- [3] J. Roberton, *J. Vac. Sci. Technol.*, 2000, 18, 1785.
- [4] A. F. Lima, J. M. Dantas, M. V. Lalic, *J. Appl. Phys.*, 2012, 112, 093709-1.
- [5] R. Jung, J. -C. Lee, Y. -W. So, T. -W. Noh, S. -J. Oh, J. -C. Lee, H. -J. Shin, *Appl. Phys. Lett.*, 2003, 83, 5226.
- [6] K. Limmer, M. Neupane, R. Brennan, and T. Chantawansri, *J. Am. Ceram. Soc.*, 2016, 99, 4007.
- [7] S. M. Hosseini, H. A. R. Aliabad, A. Kompany, *Eur. Phys. J. B*, 2005, 43, 439.
- [8] T. Ishizaka, Y. Kurokawa, *J. Lumin.*, 2001, 92, 57.
- [9] T. Ishizaka, Y. Kurokawa, T. Makina, Y. Segawa, *Opt. Mater.*, 2001, 15, 293.
- [10] T. Yang, H. Wang, M. K. Lei, *Mater. Chem. Phys.*, 2006, 95, 211.
- [11] N. Rakov and G. S. Maciel, *J. Lumin.*, 2007, 127, 703.
- [12] Vienna *ab initio* Simulation Package(VASP), Technische Universities Wein 1999.
- [13] J. P. Perdew, K. Burke, and M. Ernzerhof, *Phys. Rev. Lett.*, 1996, 77, 3865.
- [14] H. J. Monkhorst and J. D. Pack, *Phys. Rev. B*, 1973, 13, 5188.
- [15] M. Gajdos, K. Hummer, G. Kresse, J. Furthmuller, and F. Bechstedt, *Phys. Rev. B*, 1976, 73, 045112.
- [16] J. Lewis, D. Schwarzenbach, H. Flank, *Acta. Crystallogr. A*, 1982, 38, 733.
- [17] W. Y. Ching, L. Ouyang, P. Rulis, and H. Yao, *Phys. Rev. B*, 2008, 78, 014106.
- [18] R. H. French, *J. Am. Ceram. Soc.*, 1990, 73, 477.
- [19] R. Ahuja, J. M. Osorio-Guillen, J. S. Almeida, B. Holm, W. Y. Ching, and B. Johansson *J. Phys. Condens. Mat.*, 2004, 16, 2895.
- [20] B. Ealet, M. H. Elyakhlouffi, E. Gillet, and M. Ricci, *Thin Solid Films*, 1994, 250, 92.

- [21] R. Jung, J. -C. Lee, Y. -W. So, T. -W. Noh, S. -J. Oh, J. -C. Lee, H. -J. Shin, *Appl. Phys. Lett.*, 2003, 83, 5226.
- [22] J. M. Dantas, A. F.Lima, M. V. Lalic, *J. Phys.: Conference Series*, 2010, 249, 012036.
- [23] H. A. R. Aliabad, S. Ghorbani, *J. Mod. Phys.*, 2011, 2, 158.
- [24] H. A. R. Aliabad, M. Benam, H. Arabshahi, *Int. J. Phys. Sci.*, 2009, 4, 437.
- [25] A. K. Harman, S. Ninomiya, S. Adachi, *J. Appl. Phys.*, 1994, 76, 8032.
- [26] S. D. Mo, W. Y. Ching, *Phys. Rev. B*, 1998, 57, 15219.